

Beam optics and isocenter property of SC200 proton therapy gantry

Ming Li^{1,2} · Jin-Xing Zheng^{1,2} · Yun-Tao Song^{1,2} · Xian-Hu Zeng^{1,2} · Jun-Sheng Zhang^{1,2} · Wu-Quan Zhang¹

Received: 21 June 2017 / Revised: 13 October 2017 / Accepted: 19 October 2017 / Published online: 4 July 2018
© Shanghai Institute of Applied Physics, Chinese Academy of Sciences, Chinese Nuclear Society, Science Press China and Springer Nature Singapore Pte Ltd. 2018

Abstract Studies on beam optics and the isocenter property in the gantry system for the SC200 (Superconducting Isochronous Cyclotron of 200 MeV in Hefei, China) are presented in this paper. The physical design of the isocentric gantry system is developed with the software TRANSPORT, which realizes a beam with a circular shape at the isocenter and a full width at half maximum of 4–10 mm. For stereotactic radiosurgery, the isocenter deviation of the gantry system should be less than 1 mm in diameter. In order to explore the property of the isocenter, an electromagnetic structure coupling analysis has been conducted given the self-gravity and the electromagnetic (EM) force of the magnets on the gantry beam line. The correlation between the isocenter property and the EM force has also been carefully studied. This paper puts forward two methods to obtain the isocenter deviation based on the characteristics of the nozzle installation structure and the calculation of the optical path after the nozzle, respectively. The results show that the maximum isocenter deviation is less than 0.33 mm with a safety factor of 1.5, and the deviation caused by the EM force is 0.05 mm. The latter result indicates that the impact of the EM force is negligible. This paper puts forward one possible way to realize real-time acquisition of the isocenter deviation in

practical application. The gantry of SC200 is under construction at ASIPP.

Keywords Beam optics · Isocentric gantry · Optical path calculation · Coupled analysis

1 Introduction

A gantry is the final section of a proton therapy facility (PTF). Its function is broadening the scope of treatment and offering a comfortable positioning for patients. From a design point of view, the most important requirement is to ensure the accuracy of the mechanical isocenter of the gantry, which should be less than 1 mm [1]. At an early stage of the design phase, a corkscrew-type gantry [2] and an eccentric-type gantry [3] are proposed and constructed. The practical experience indicates that the former has a large bend radius and the latter puts geometrical constraints on the available treatment angles. Thus, these defects limited the development of both kinds of structures. A cantilever-type structure was adopted in the PSI gantry 2 [4]. Given the rotating gantry used for CIRT [5], the PSI gantry 3 [6] was also modified to introduce an isocentric structure. In this way, the gantry becomes lighter, and the control of the accuracy of the isocenter becomes easier.

The gantry system of the SC200 [7] (Superconducting isochronous cyclotron of 200 MeV in Hefei, China) proton therapy device adopts an isocentric structure, which accommodates very heavy non-superconducting magnets with an ampere-turn of approximately 50 kA. As a result, the gantry deformation may be influenced by the electromagnetic (EM) force of the magnets. The existing literature mainly focused on measurements [8–11] under down state

This work was supported in part by the National Natural Science Foundation of China (No. 51507173).

✉ Jin-Xing Zheng
jxzheng@ipp.ac.cn

¹ Institute of Plasma Physics, Hefei Institutes of Physical Science, Chinese Academy of Sciences, Hefei 230031, China

² University of Science and Technology of China, Hefei 230031, China

and ignored the electromagnetic property of gantry magnets [12] during the beam transport.

The optical design of the gantry beam line in SC200 is calculated with the software TRANSPORT [13] and presented in this paper. Such design mainly focuses on the correlation between the electromagnetic property and the isocenter property. The impact of the EM force on the gantry deformation is analyzed with union simulation [14, 15] at selected gantry angles. We analyzed the deformation and plane rotation of the nozzle installation plate on the gantry, by respecting the requirements on the accuracy of the isocenter. The optical path coming out from this analysis is also calculated to determine the actual isocenter position based on the deformation of the nozzle and the beam property. Such research will be of great significance for the design and construction of the gantry in the SC200 project.

The paper consists of four parts. Part 1 introduces the physical design of the gantry. Part 2 describes the process of the electromagnetic structure coupling analysis. Part 3 explains the two methods used to obtain the isocenter deviation. In part 4, the results are compared and the final conclusions are drawn.

2 Experimental section

2.1 Physical design of SC200 gantry

The design of the gantry structure depends on the optical design of the beam line. This means that the optical parameters of the gantry beam line should be carefully selected and optimized in order to design the most compact gantry. The position of horizontal and vertical planes is swapped due to rotation. This is required to ensure the same beam characteristics on both planes at the entrance. Moreover, the isocenter will not change with rotation in order to make the beam delivery of the gantry independent of the rotating angle of the gantry itself and, thus, simplify the design of the beam optics.

The paper presents a new optical design of the isocentric gantry, which is calculated with the software TRANSPORT. The principle of beam line inversion (BLI) is adopted to design the optics of the gantry beam according to the requirements on the isocenter beam. The initial conditions concern the shape of the beam and its energy: the shape is circular at the isocenter, with a full width at half maximum (FWHM) of 4–10 mm, and the energy varies in the range 70–200 MeV. The beam is deflected with three magnets (AMD3 90°, AMD2 60°, AMD1 60°) and focused by seven quadrupoles (QMD1–QMD7). The layout of the gantry beam line is shown in Fig. 1. The beam envelope of the first-order beam optics calculation of the

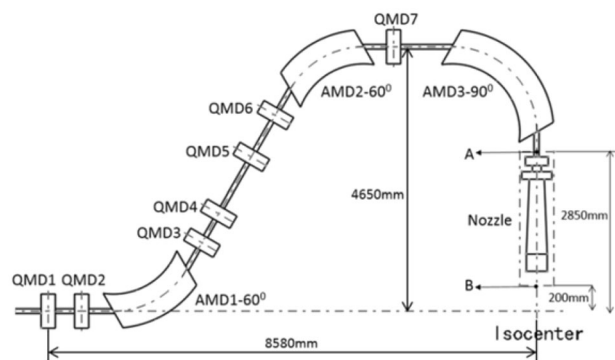


Fig. 1 Layout of the SC200 gantry beam line

SC200 gantry is shown in Fig. 2. The main parameters of the gantry beam line are summarized in Table 1. Considering the proton beam energy and the maximum magnetic field that the magnets can reach, the bending radius of the gantry magnets is set to be 1.5 m. The edge angle is 30° for each bending magnet, and the effective length of the quadrupole is 0.25 m.

Based on the optical design of the gantry beam line, the gantry of the SC200 PTF is designed taking into consideration the space of the treatment room and the construction cost. The main design element is the basic cylinder structure, which allows a more uniform stressing and a lower weight. The maximum and minimum diameters of the cylinder structure are 5000 and 4400 mm, respectively. The three-dimensional (3D) model of the gantry is shown in Fig. 3. Two support rings are installed on both ends of the gantry at a distance of 7850 mm between the two. The main support is a self-centering multi-wheels structure.

Bonded yokes should be connected to the gantry. During the beam transport, the direction of the EM force remains unchanged against the structure of gantry, whereas its relative direction and self-gravity change with the rotation of the gantry. Hence, the integrated load changes synchronously.

2.2 Electromagnetic structure coupling analysis

As far as the PTF concerns, various beam energies are needed to ensure an effective radiation of tumors located at different depths. On account of the fact that the rotation radius is constant, the field of dipoles should change according to the beam energy. The correlation between the field intensity and the beam energy is described by Eq. (1). The higher the beam energy, the higher the magnetic field needed to maintain a constant radius. Therefore, as to the EM force analysis, it is necessary to focus only on the maximum input currents, which are summarized in Table 2. The seven quadrupoles are classified by magnetic field gradient (the threshold is 12 T/m) into two groups.

Fig. 2 (Color online) Beam envelope of the gantry (first-order beam optics calculation for the SC200 gantry). The curve in the upper (lower) part of the plot represents the vertical (horizontal) envelope. The dotted line indicates the 1%-dispersion trajectory

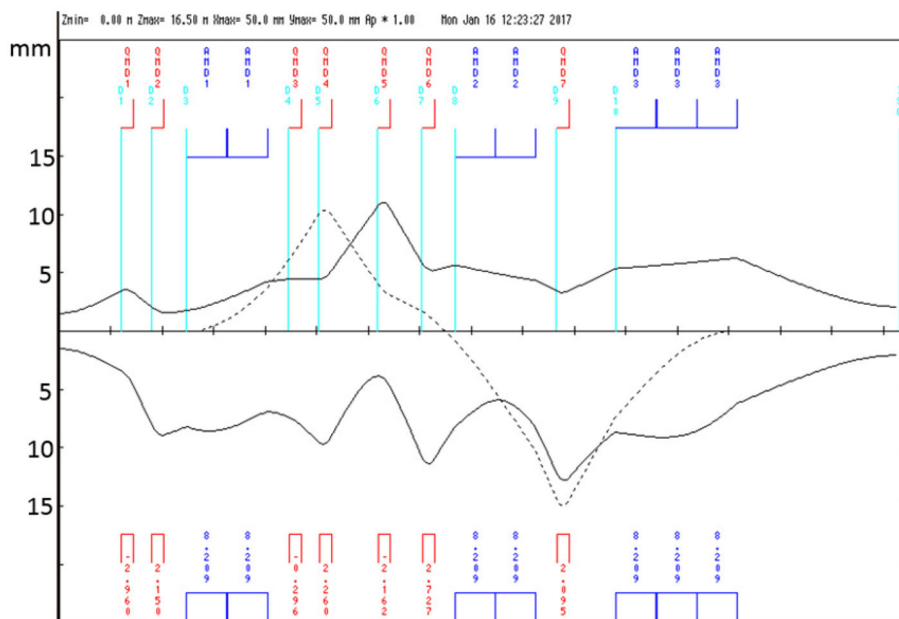


Table 1 Major parameters of the gantry beam line

Parameters	Value
Maximum momentum spread of gantry (%)	0.8
Maximum beam envelope (mm)	27.14
Coupling point matching parameter (°)	$\alpha = 0, \beta = 0.608$
Radius of gantry beam line (m)	4.65
Length of gantry beam line (m)	9.6
FWHM at isocenter (mm)	4–10
Energy range (MeV)	70–200
Maximum emittance (π mm mrad)	16
Delivery	PBS
Field size (cm^2)	30×40
Rotation angle (°)	± 185

Quadrupoles of the same group adopt the same mechanical structure.

$$B = \frac{m}{qr} \sqrt{\frac{2E}{m}} \quad (1)$$

With consideration of the magnet design and beam motion, the direction of the input current is specific for each magnet. All the magnets are analyzed separately for EM force coupling. In order to map the EM force consistently, the global coordinate system of the analysis model must be the same in both Maxwell and ANSYS Workbench simulation environments. The total force is shown in purple in Fig. 4. As can be seen, the EM force of the beam line magnets is mainly reflected in the x and z directions of the

dipoles AMD-3, AMD-2, and AMD-1, with an intensity of 50.97, 49.29, and 49.18 kN, respectively.

Given the complex structure of the nozzle, an alternative model is adopted. The simplified model consists of a skeleton, scan magnets, an ionization chamber (IC) and an outer support plate for the nozzle, whose stiffness and weight are almost the same as the real nozzle. The distance between the end of the last bending magnet and the isocenter is 2850 mm, including the 2650-mm nozzle length and the 200-mm air path, which are both shown in Fig. 1.

The 90° dipole and the 60° dipoles have a weight of 13 and 6.5 t, respectively. Quadrupoles of the first and second group have a weight of 0.5 and 0.8 t, respectively. The total weight of the gantry is 130 t. The weight ratio can reduce the impact of magnets weight on the gantry deformation. Therefore, the deformation of the gantry at different positions can be more uniform and controllable.

In order to simplify the analysis, the following key gantry angles are selected: 0°, ± 45°, ± 90°, ± 135°, 180°. The gantry shown in Fig. 3 is at 0°. Fixed constraints have been applied to both ends of each support wheel. Two load steps are adopted to analyze the impact of the self-gravity and the EM force. The total deformation after load step two at 0° is shown in Fig. 5. The maximum deformation occurs in the middle position of the gantry, which is 0.26 mm. The maximum equivalent stress, which occurs in the contact position between the support ring and the support wheel, is equal to 47.79 MPa. Figure 6 shows the maximum deformation of two load steps at the selected gantry angles. The maximum deformation always occurs in correspondence of the position of the 90° dipole. The deformation is

Fig. 3 (Color online) 3D model of the gantry. The system of global coordinates used is shown on the top-left corner of the figure

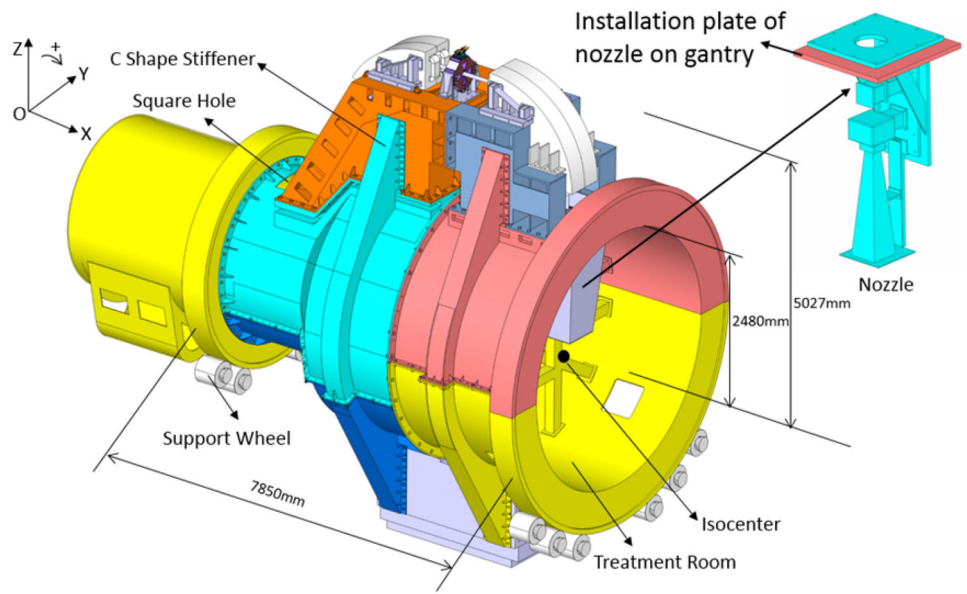


Table 2 Parameters of beam line magnets (negative sign means inverse current)

Magnets	Serial no	Ampere-turns (A)	Magnetic field gradient	Magnetic field
Dipole	AMD-1	51,702.48	–	1.433
	AMD-2	51,702.48	–	1.433
	AMD-3	51,702.84	–	1.433
Quadrupole	QMD-1	– 5248.32	– 7.13	–
	QMD-2	6226.80	8.46	–
	QMD-3	11,913.00	16.19	–
	QMD-4	– 9018.40	– 12.26	–
	QMD-5	5180.56	7.05	–
	QMD-6	4428.48	6.02	–
	QMD-7	8578.08	11.66	–

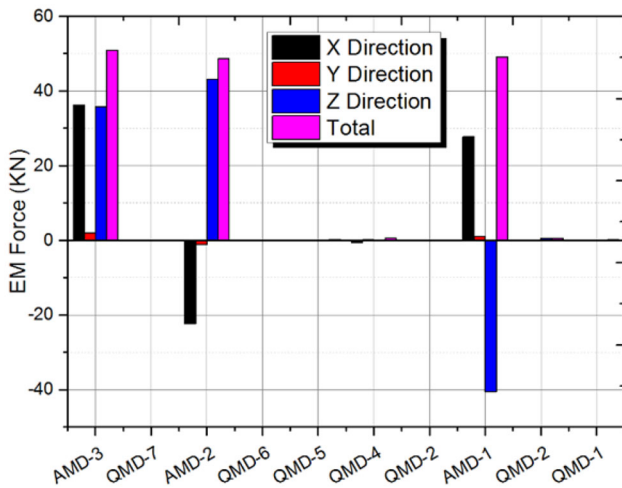


Fig. 4 (Color online) EM force of beam line magnets

symmetrical with respect to the $x-z$ plane, and it results to be less than 1 mm for all runs.

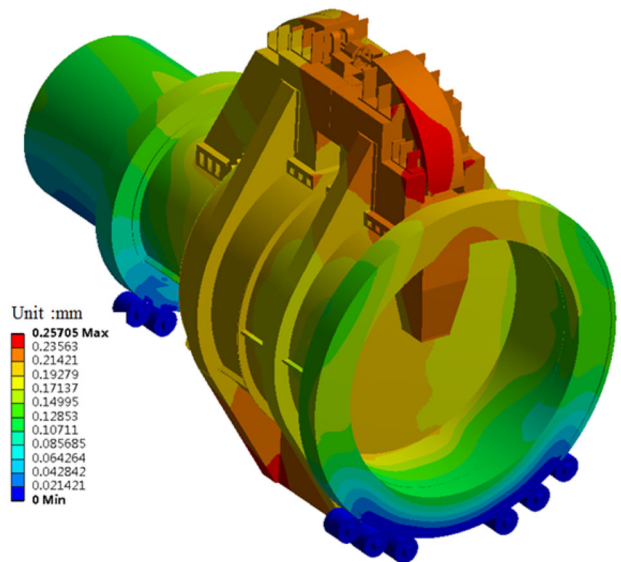


Fig. 5 (Color online) Total deformation of the gantry at 0° after load step two

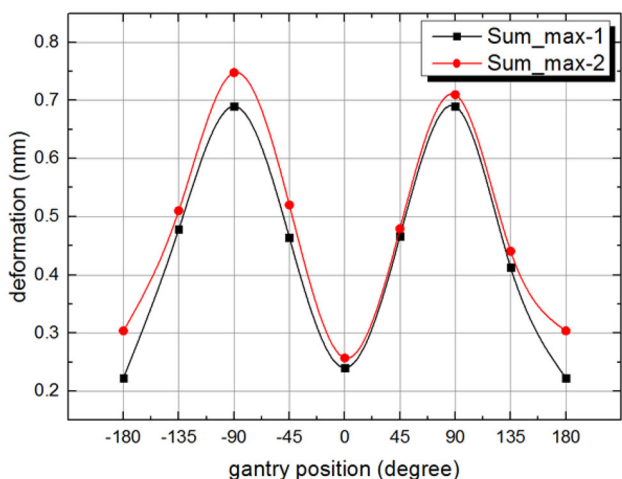


Fig. 6 (Color online) Maximum deformation of gantry at selected angles (square symbols represent the results after load step 1 and circle symbols represent the results after load step 2)

3 Methods to obtain isocenter deviation

3.1 Method one: based on the nozzle installation

After understanding the deformation of the nozzle structure and the beam trajectory, we can calculate the optical path coming out of the nozzle. Theoretically, the isocenter is the intersection between the axis of the nozzle and the rotating axis of the gantry. Due to the deformation of the gantry and the nozzle, the actual isocenter is a region in space whose shape can be defined as the path of a point that is on the central axis of the beam delivery system and at a constant distance from the target (or scatterer), as the gantry rotates through its entire range of motions. Therefore, the isocenter size cannot be obtained directly.

To determine the size of the isocenter, the deformation data of the points A and B of the nozzle, as indicated in Fig. 1, are obtained directly. Such two points are on the axis of the nozzle. The distance between the point A and the isocenter is 2850 mm, whereas the distance between the point B and the isocenter is 200 mm. When the beam comes out of the nozzle from point B, it arrives at the practical isocenter through the same distance along the original direction of the motion at any gantry angle. Given this, the optical path coming out of the nozzle may be calculated to obtain the practical coordinate value of the isocenter in the global coordinate system.

3.2 Method two: based on the optical path after nozzle

The requirement of having the nozzle on the mechanical deformation of the gantry is essential for the gantry design. The scanning system and the ICs are placed on a rigid

subplate, which maintains the relationship between magnets and ICs. Given the complexity of the nozzle system, the nozzle can be assumed to be perfectly rigid. Therefore, we can confine the attention on the location of the subplate relative to the rest of the gantry and look at the effects of the offsets in various axes. Figure 7 shows a scheme of a scan magnet deflecting a beam and an IC rigidly connected to the magnet. The chamber is represented with a deliberately exaggerated shift with respect to the beam path defined by the gantry, which is assumed to be perfect.

In all cases, the actual deflection of the beam is hardly affected, but the positions measured by the ionization chamber. By comparing the case (a) with the case (b) in Fig. 7, it can be observed that the shift in the z direction has a negligible effect on the beam line because the deflection angles are small. The shift in the $x(y)$ direction brings the IC to measure the beam in the wrong position, even though the deflection in the magnet remains unchanged. The beam lines B and D pass through different positions of the IC. The position of the beam is wrongly measured when the $x-z$ ($y-z$) plane is deflected; a deflection that results in a shift in the $x(y)$ direction.

The requirement of rigidity imposed on the mounting of the nozzle is no worse than the same requirement imposed on other transfer line magnets on the gantry. Given that a typical requirement for spot placement accuracy at the isocenter plane is ± 0.5 mm (pure mechanical accuracy), and a typical demagnification is about 1.6, the scan system subplate should be maintained in a position relative to the nominal beam trajectory that has to be better than 0.3 mm in x and y . The rotation in the planes $x-z$ and $y-z$ should be kept below about 0.3 mrad. The safe factor is set equal to 1.5. The requirements on the installation plate are expressed in Eq. (2). In this case, the local coordinate system is considered.

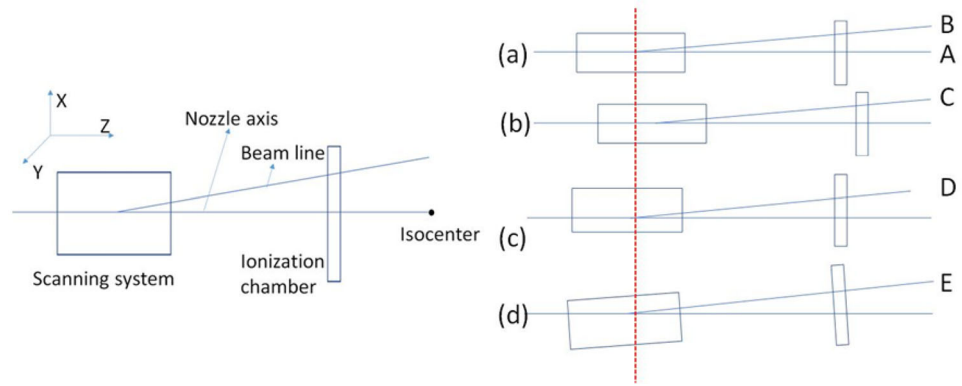
The rotation angle in the $x-z$ plane is calculated with Eq. (3), where z_{\max} and z_{\min} represent the maximum and minimum deformation in the z direction, respectively; l_x and l_y ($l_x = 1020$ mm, $l_y = 1100$ mm) are the dimensions of the nozzle installation plate on the gantry in the x and y directions, respectively.

$$\begin{aligned}
 |x_{\max}| &\leq 0.2 \text{ mm} \\
 |y_{\max}| &\leq 0.2 \text{ mm} \\
 |\theta(xz)_{\max}| &\leq 0.2 \text{ mrad} \\
 |\theta(yz)_{\max}| &\leq 0.2 \text{ mrad}
 \end{aligned}
 \tag{2}$$

$$\begin{aligned}
 \theta(xz) &= \frac{z_{\max} - z_{\min}}{l_x} \\
 \theta(yz) &= \frac{z_{\max} - z_{\min}}{l_y}
 \end{aligned}
 \tag{3}$$

Assuming that the nozzle is perfectly rigid, we can get the equivalent isocenter deformation from the deformation

Fig. 7 Scheme of the nozzle system: (a) normal condition; (b) shift in the z direction; (c) shift in the $x(y)$ direction; (d) rotation in the $x-z(y-z)$ plane



and the rotation of the nozzle installation plate on the gantry. To achieve this, the relations expressed by Eq. (4) have to be used.

$$\begin{aligned}
 x_{\text{iso_equi}} &= x_{\text{max}} \pm l\theta(xz) \\
 y_{\text{iso_equi}} &= y_{\text{max}} \pm l\theta(yz) \\
 z_{\text{iso_equi}} &= z_{\text{max}}
 \end{aligned}
 \tag{4}$$

Here $x_{\text{iso_equi}}$, $y_{\text{iso_equi}}$ and $z_{\text{iso_equi}}$ are the equivalent isocenter deformations in the x , y and z directions, respectively. $\theta(xz)$ and $\theta(yz)$ can be obtained from Eqs. (2) and (3). l is the distance between point A and the isocenter.

4 Results and discussion

4.1 Results

As to method one, the isocenter deformation is obtained by calculating the optical path coming out of the nozzle. The results are shown in Fig. 8. The optical path after the nozzle (200 mm long) is shown in Fig. 9.

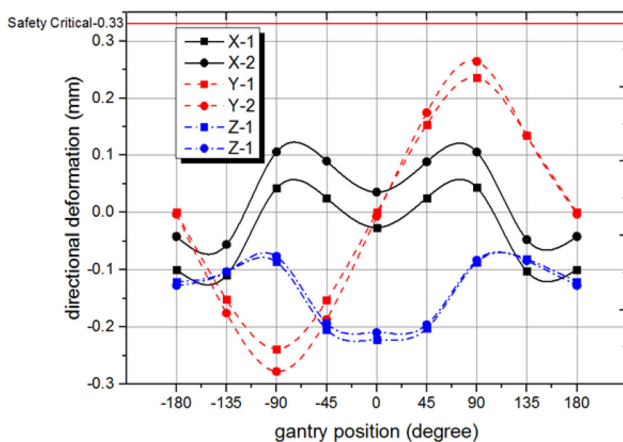


Fig. 8 (Color online) Isocenter deviation obtained with method one (*- 1 indicates the load step 1 and *- 2 indicates the load step 2)

The nozzle has a cantilever structure and, due to its own weight, the practical isocenter moves downward. The y direction deviation in the vicinity of $\pm 90^\circ$ is exactly the opposite in the global coordinate system. As we can see from Fig. 8, only the x direction deviation is affected by the EM force.

In general, the isocenter deviation in the x and y directions is less than 0.33 mm (considering a safety factor of 0.5–1.5) at selected gantry angles and the maximum linear distance between the theoretical and practical isocenter is 0.39 mm. The variation of the maximum deformation between two loads steps is 0.05 mm, which means that the EM force does not have a great impact on the isocenter deviation.

As to method two, the equivalent isocenter deformation can be obtained from the deformation data (deformation and rotation) of the installation subplate of the nozzle, which is shown in Fig. 10. In this case, the maximum deformation changes according to a regular pattern and it is symmetrically distributed along the 0° position. The rotation angle of the nozzle installation plate on the gantry is shown in Fig. 11. The maximum rotation angle is less than 0.1 mrad.

Starting from the results shown in Figs. 10 and 11, we can obtain $x_{\text{iso_equi}}$, $y_{\text{iso_equi}}$ and $z_{\text{iso_equi}}$ by using Eq. (4). It is worth to note that the relationship between the rotation and deformation directions of the nozzle installation plate, and the equivalent isocenter deformation, is converted into global coordinates for a consistent comparison with that obtained with method one. The result of such comparison is shown in Fig. 12.

As shown in Fig. 12, the difference between the isocenter deformations obtained with the two methods is quite small. Therefore, it can be neglected. In a practical application context, this means that the isocenter is a point in space, and it is difficult to determine its deformation directly. Thus, according to the results shown above, we can mount deformation-monitoring equipment on the nozzle installation plate and calculate the isocenter

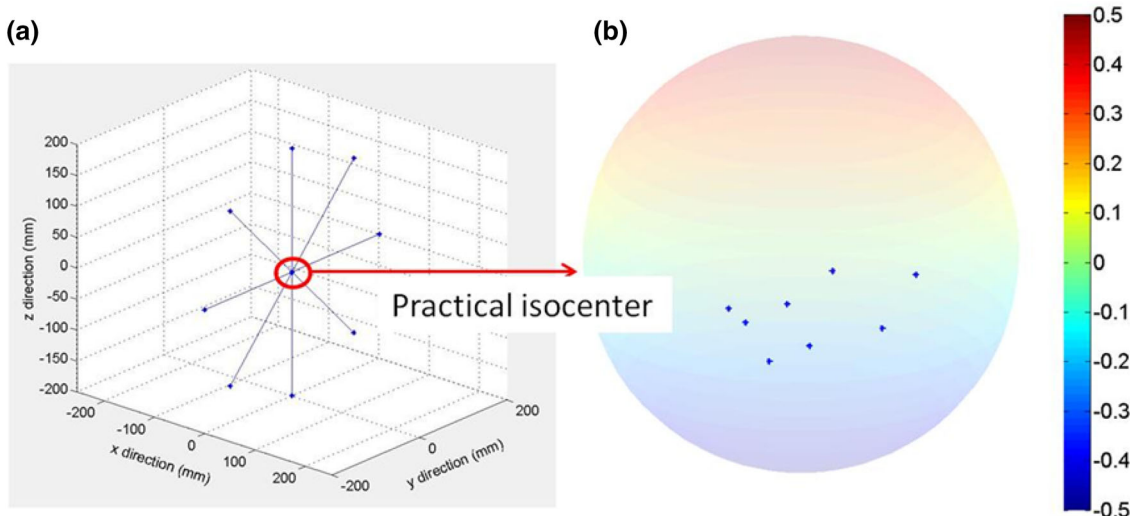


Fig. 9 (Color online) Optical path after the nozzle at selected gantry angles: **a** the middle point indicates the practical isocenter, whereas the peripheral points indicate the point B at certain selected gantry angles; **b** the practical isocenter in critical boundary

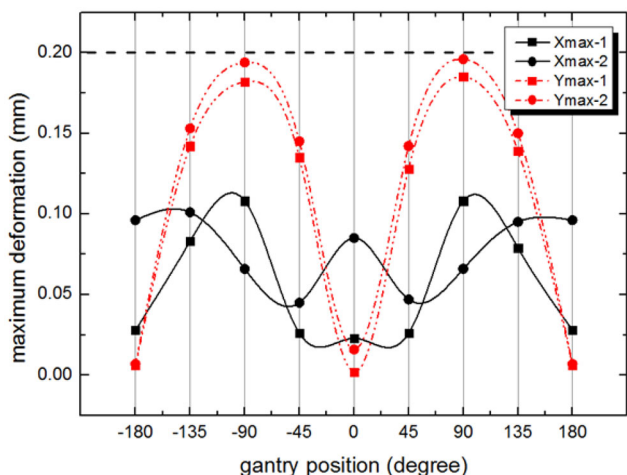


Fig. 10 (Color online) Technical parameters of the nozzle installation plate on the gantry: maximum deformation in the x and y directions (*- 1 indicates the load step 1 and *- 2 indicates the load step 2)

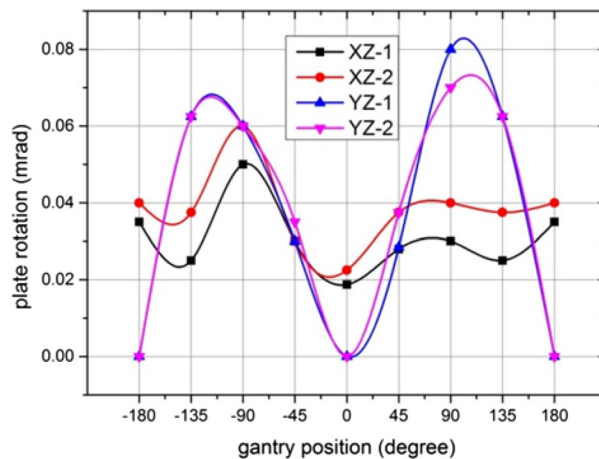


Fig. 11 (Color online) Technical parameters of the nozzle installation plate nozzle on the gantry: maximum plate rotation of the x - z and y - z plates (*- 1 indicates the load step 1 and *- 2 indicates the load step 2)

deformation by exploiting the monitoring data. Such method is applicable to realize real-time monitoring of the isocenter deformation.

5 Conclusion

An investigation of beam optics and isocenter properties of the rotating gantry for the SC200 proton therapy system has been presented in this paper. The property of the beam optics is consistent during the gantry rotation and a circular beam shape is obtained at the isocenter. The treatment field

size is 30 cm \times 40 cm and the FWHM at the isocenter is 4–10 mm.

The purpose of this paper is to explore the impact of EM force and self-gravity on the deformation of the isocenter. After having analyzed the variations of the installation plate and isocenter deformations, we concluded that the deformation on the x direction is affected by the EM force, whereas the deformation on the y and z directions is negligible. Such different impacts are due to the distribution of the EM force. The results show that there is a negligible relationship between the EM force and the isocenter property. Moreover, precise treatments can be delivered allowing a deflection of 0.5 mm if the calculated isocenter path is applied.

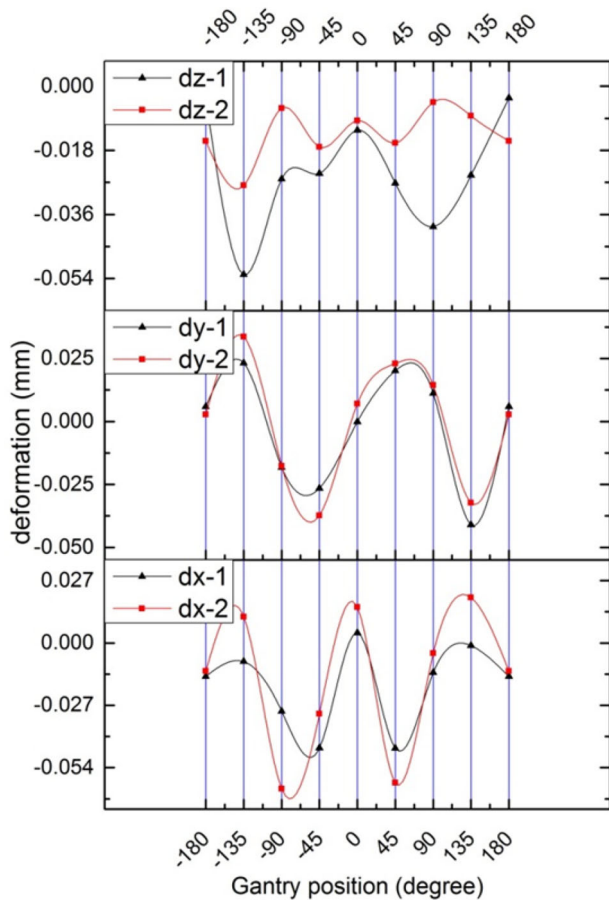


Fig. 12 (Color online) Comparison between the isocenter deformations obtained with methods one and two (*- 1 indicates the load step 1 and *- 2 indicates the load step 2)

Based on the characteristics of the nozzle and the proton beam, this paper puts forward two kinds of ways to obtain the isocenter deformation and, in addition, the calculated results show that the difference between these two ways is negligible. We presented a potential way to calculate the isocenter deformation indirectly by acquiring real-time isocenter deformation data. The gantry system of the SC200 proton therapy devices is under construction at ASIPP in Hefei, China.

References

1. H.L. Riis, S.J. Zimmermann, M. Hjelmhansen, Gantry and isocenter displacements of a linear accelerator caused by an add-on micromultileaf collimator. *Med. Phys.* (2013). <https://doi.org/10.1118/1.4789921>
2. A.M. Koehler, Preliminary design study for a corkscrew gantry, in *Proceedings of the Fifth PTCOG Meeting: International Workshop in Biomedical Accelerators* (Lawrence Berkeley Laboratory, Berkeley, CA, 1987), p. 147
3. E. Pedroni, T. Böhringer, A. Coray et al., A novel gantry for proton therapy at the Paul Scherrer Institute. *AIP Conf. Proc.* **600**, 13–17 (2001). <https://doi.org/10.1063/1.1435184>
4. E. Pedroni, R. Bearpark, T. Böhringer et al., The PSI gantry 2: a second generation proton scanning gantry. *Z. Med. Phys.* **14**, 25–34 (2004). <https://doi.org/10.1078/0939-3889-00194>
5. Y. Iwata, T. Fujimoto, S. Matsuba et al., Beam commissioning of a superconducting rotating-gantry for carbon-ion radiotherapy. *Nucl. Instrum. Methods Phys. Res. A* **834**, 71–80 (2016). <https://doi.org/10.1016/j.nima.2016.07.050>
6. A. Koschik, C. Baumgarten, C. Bula et al., PSI gantry 3: integration of a new gantry into an existing proton therapy facility, in *7th International Particle Accelerator Conference (IPAC 16)*, JACOW, Geneva, Switzerland (2016), pp. 1927–1929
7. G. Karamysheva, Y. Bi, G. Chen et al., Compact superconducting cyclotron SC200 for proton therapy, in *Proceedings of Cyclotrons and their Applications 2016*, Zurich, Switzerland, pp. 371–373
8. X. Ding, M. Bues, M. Zhu et al., SU-FF-T-291: measurement of the mechanical isocenter of a proton gantry. *Med. Phys.* **34**, 2468 (2007). <https://doi.org/10.1118/1.2760953>
9. S. Price, S. Goddu, L. Rankine et al., SU-E-J-213: imaging and treatment isocenter verification of a gantry mounted proton therapy system. *Med. Phys.* **41**, 206 (2014). <https://doi.org/10.1118/1.4888266>
10. H. Schiefer, N. Ingulfsen, J. Kluckert et al., Measurements of isocenter path characteristics of the gantry rotation axis with a smartphone application. *Med. Phys.* **42**, 1184 (2015). <https://doi.org/10.1118/1.4906248>
11. M.F. Moyers, W. Lesyna, Isocenter characteristics of an external ring proton gantry. *Int. J. Radiat. Oncol. Biol. Phys.* **60**, 1622–1630 (2004). <https://doi.org/10.1016/j.ijrobp.2004.08.052>
12. P. Spiller, D. Boehne, A. Dolinskii et al., Gantry studies for the proposed heavy ion cancer therapy facility in Heidelberg, in *Proceedings of 7th European Particle Accelerator Conference (EPAC)*, Cern, Geneva (2000), pp. 2551–2553
13. D.C. Carey, K.L. Brown, F. Rothacker et al., TRANSPORT, a computer program for designing charged particle beam transport systems, SLAC Report No. SLAC-R-95-462
14. X. Zhang, W. Fan, S. Shi et al., Average vector method for determining isocenter of rotated radiotherapy equipment. *J. Tsinghua Univ.* **8**, 470–472 (2015)
15. T. Obana, T. Ogitsu, Magnetic field and structure analysis of a superconducting dipole magnet for a rotating gantry. *Physica C* **471**, 21–22 (2011). <https://doi.org/10.1016/j.physc.2011.05.213>